

High Current Dispersion Effect

G. Franchetti, I. Hofmann, S. Lund¹
¹ LLNL

In 1998 the High Current Acceleration Group has focused its work on completing the HIDIF (Heavy Ion Driven Inertial Fusion) Report [1], investigations in connection with a future GSI facility, and beam physics studies in circular machines under conditions of high space charge. An important focus in the discussion of a new accelerator facility at GSI has been the advancement of plasma physics target experiments to significantly higher bunch energies (10's of kJ) and target temperatures (30-100 eV). A 100 Tm ring as a preliminary machine is considered. The constrain in the design was of using the same technology developed for SIS18 where dipole magnets have a maximum field of 1.8 Tesla and where the maximum gradient for the quadrupoles of ~ 11.2 Telsa/m². These requirements reduce the phase phase advance per cell due the increase of the rigidity. A compromise between maximize the acceptance and keep the machine tunes below systematic resonances brought to the test ring sketched in Fig 1. Other parameters of this ring are superperiodicity

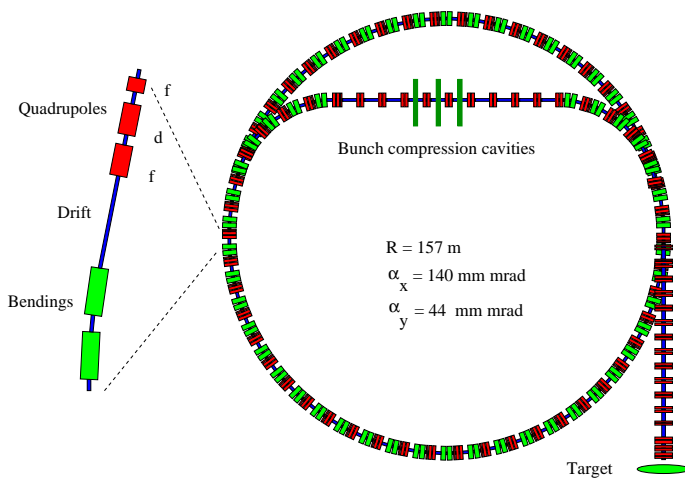


Figure 1: SIS100 lattice for fast compression scheme.

50 and the tunes $q_x = 10.8$, and $q_y = 9.7$. A major challenge in these studies is the computer modeling of bunch compression in such a facility and the issue of emittance growth in the presence of dispersion and space charge.

1 Dispersion and Space Charge Effects in Rings

Fast bunch rotation schemes call for the compression of an initially prebunched beam in a ring with a momentum spread of $\Delta p/p \sim 10^{-4}$ to a final spread of $\Delta p/p \simeq 1\%$ at the final focus optic. The transverse space-charge strength and incoherent momentum spread at mid-pulse rapidly increase during the final phase of this compression. For the range of rings considered, this compression takes place over 50-150 laps and, in the absence of transverse emittance dilution, results in 1-4 integers of space-charge

induced tune shift at peak compression. This combination of strong transverse space-charge strength and large momentum spread in the ring and the extraction line to the target lead to numerous issues in maintaining transverse beam focusability (i.e., limiting emittance growth). These issues are essentially the same whether the compression is implemented by RF or induction technology and are being explored with a hierarchy of two- and three-dimensional electrostatic PIC simulations employing codes developed at GSI and LLNL[2]. These simulations include lattices with varying levels of detail, a proper treatment of dispersion, and self-consistent space-charge fields. The focus has been on identifying and understanding emittance growth processes as opposed to evaluating detailed designs.

A simulation of a characteristic mid-pulse rms emittance evolution is shown in Fig. 2 for a 180° phase-space rotation (over 120 laps) in an 18 Tesla-meter FODO ring with strong space-charge parameters. This simulation was produced by the WARP code developed at LLNL agrees with micro-map (MIMAC) and PIC simulations with GSI codes. Fig. 3 shows a compression (90°, 50 laps) for SIS100 produced by MIMAC code. The in-bend-plane (Fig. 2) x -emittance undergoes a large increase at peak compression (90°, 60 laps), whereas the out-of-bend y -emittance undergoes a smaller, nonlinear space-charge driven increase. The thickness of the x -emittance (Fig. 2, Fig. 3) trace indicates the amplitude of emittance oscillations at the particle betatron frequency that are induced by the (initially matched) distribution being dispersion mismatched due to the bunch compression. The envelope of oscillations moves up as the compression-pumped momentum spread increases. In the absence of space charge, resonance effects, etc., such emittance growth induced by distribution distortions represents correctable, "reversible" growth. Such a correction can be implemented by extracting the beam at a dispersion function null point or bending the extraction line appropriately to correct the distortion. With space-charge, resonances, etc., a component of this growth is thermalized in the distribution and represents "irreversible" growth. Such irreversible growth must be understood and controlled since it can interfere with the correction of the large, reversible growth component. The increases in emittance at the 180° rotation point (Fig. 2) provides a measure of the irreversible growth, since the momentum spread is approximately the initial value at this point. The simulations produced for SIS100, due to its systematic-resonance free design, did not exhibit irreversible growths. Fig. 3a),c) show also the evolution of the rms transverse beam sizes versus ring laps.

Preliminary considerations suggest that the following processes are issues of concern:

- Nonlinear space-charge forces, chromaticity in focusing elements, and possibly additional processes phase-mixing otherwise reversible distribution distortions

into irreversible growth.

- Space-charge leading to a broadening and mismatch seeding of envelope instabilities associated with high phase advance parameters sometimes employed for increased dynamic aperture.
- Discrete kicks from bunching cavities/cells when placed at points of nonzero dispersion.

Other issues such as space-charge induced resonance crossings, dispersion induced integer resonance crossings, and transverse/longitudinal coupling seem to be less problematic. Progress has been made, but continued work is necessary to better understand these processes (which are not fully decoupled) and determine reliable design criteria.

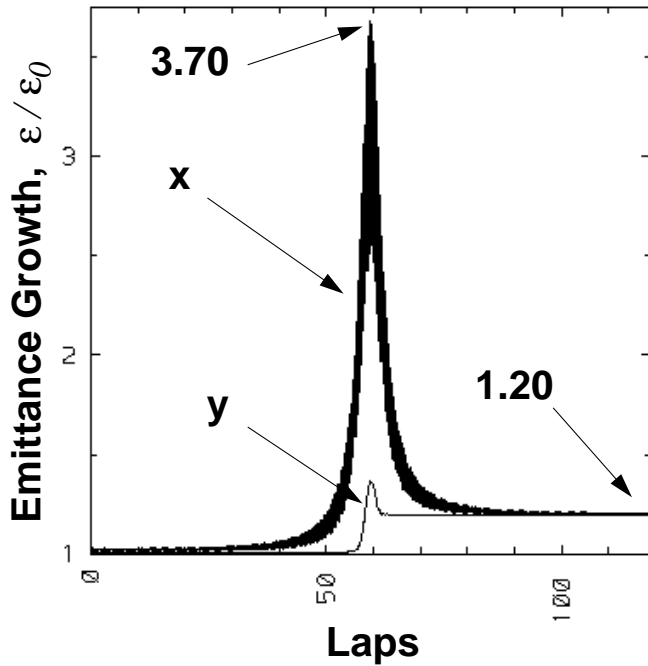


Figure 2: RMS emittance growth versus ring laps of the bunch centroid for SIS18.

References

- [1] *The HIDIF-Study*, eds. I. Hofmann and G. Plass, GSI-98-06 (1998)
- [2] S. Lund, I. Hofmann, O. Boine-Frankenheim, G. Franchetti, P. Spiller, "Simulations of Axial Bunch Compression in Heavy Ion Rings for Plasma Physics Applications at GSI," to appear in *Proceeding of the 1999 Particle Accelerator Conference*, New York City, USA, 29 March - 2 April, 1999.

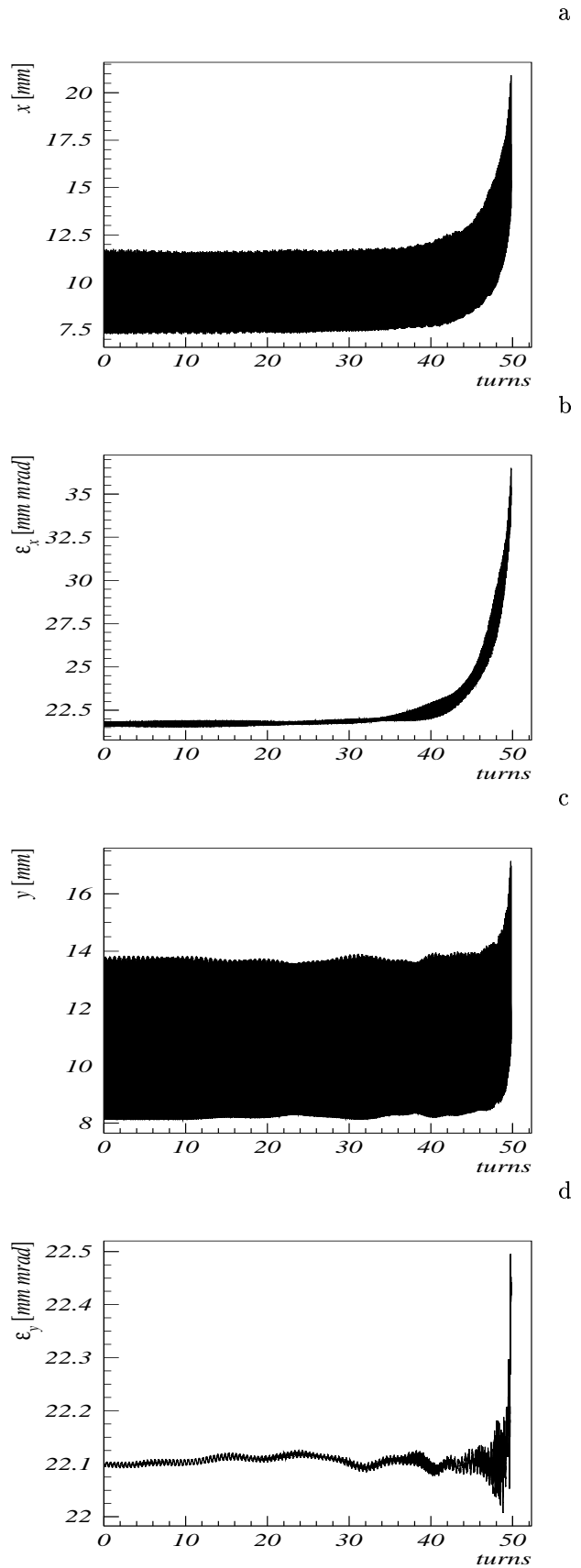


Figure 3: a) RMS x size; b) RMS emittance; c) RMS y size; e) RMS emittance size.